Eur. Phys. J. C (2016) 76:342
DOI 10.1140/epjc/s10052-016-4191-9

THE EUROPEAN PHYSICAL JOURNAL C

Regular Article - Theoretical Physics

Soft wall model for a holographic superconductor

S. S. Afonin[a], **I. V. Pusenkov**[b]

Saint Petersburg State University, 7/9 Universitetskaya nab., St.Petersburg 199034, Russia

Received: 5 August 2015 / Accepted: 9 June 2016 / Published online: 20 June 2016

Abstract We consider the soft wall holographic approach for description of the high-T_c superconductivity. In comparison with the existing bottom-up holographic superconductors, the proposed approach is more phenomenological and does not describe the superconducting phase transition. On the other hand, technically it is simpler and has more freedom for fitting the conductivity properties of the real high-T_c materials in the superconducting phase. Some examples of emerging models are analyzed.

1 Introduction

The holographic description of the high-T_c superconductors has become an important application of the AdS/CFT correspondence [1,2] in condensed matter [3–5]. The active research in this field was inspired by an observation made in Ref. [6] that certain holographic models could describe the high-T_c superconductivity discovered in some cuprates and other materials. This enigmatic phenomenon has still not been understood [7]. It is not described by the standard BCS theory (a theory of weak inter-fermion interactions mediated by phonons) since it seems to be caused by a strong coupling between fermions [8]. Due to the strong coupling the establishing of the ground state of the system becomes a hard problem. This state is not the Fermi liquid as in the BCS theory.

It must be emphasized that the high-T_c superconductors represent much more complex materials than the usual superconductors. Aside from the layered structure, the critical temperature depends crucially on the so-called doping parameter, let alone a strong dependence on the external pressure [7]. The onset of the superconducting phase seems to have a very different nature in the underdoped and overdoped regions. In the latter region, one has the pairing mechanism partly like in the conventional superconductors. In the underdoped domain, the superconducting phase appears due to phase ordering: because of very small density of charge carriers, the emergence of superconducting condensate is determined not by formation of Cooper-like pairs but by beginning of phase correlations among already existing pairs. In addition, in the high-T_c materials, the instability of Fermi surface is not only due to superconducting phase (as in the case of usual superconductors) but also due to various other collective ordering phenomena which compete with superconductivity [7].

The first holographic superconductor was constructed in Ref. [6] and further developed in Ref. [9]. It ignored all these complications and described the high-T_c superconductivity in the spirit of Ginzburg–Landau theory of superconductivity. The model represents just an Abelian–Higgs bottom-up holographic model with black hole. All other bottom-up holographic superconductors proposed in the literature can be viewed as extensions of the model of Ref. [6]. The existing holographic models, both in the bottom-up and in the top-down approaches, give only a rough qualitative description of the real high-T_c materials.

From the point of view of a condensed matter phenomenologist, it would be interesting to have a simple holographic superconductor with several adjustable parameters which would allow to fit the physical characteristics of a concrete superconducting material. Our aim is to propose such a model. Since the nature of high-T_c superconducting phase transition is complex and very far from complete understanding we will not attempt to provide a simple model for the phase transition itself. By assumption, our model will describe the superconducting phase only, namely the behavior of optical conductivity and perhaps other observables.

The idea of our approach is borrowed from the soft wall (SW) holographic model in hadron physics [10]. The purpose of construction of the SW model was essentially the same – advancing in quantitative holographic description of

[a] e-mail: s.afonin@spbu.ru

[b] e-mail: i.pusenkov@spbu.ru

real experimental data. The SW model is well tunable for description of the hadron spectra and related phenomenology, albeit it does not describe (at least in its simplest version) the spontaneous chiral symmetry breaking in QCD – by assumption, the model is formulated in the phase where the chiral symmetry is already broken. Our SW holographic superconductors will be also quite flexible for fitting the observable properties of high-T_c superconductors, first of all the behavior of optical conductivity. However, we need to pay a similar price – the simplest SW superconductor does not describe the superconducting phase transition. Embedding this description seems to require nontrivial complications. But if we are interested in a description of experimentally measurable quantities, the approach that we propose should be considered as a step forward to building a phenomenologically useful holographic description of high-T_c superconductors.

The structure of the paper is as follows. In order to make the text self-contained and to help in comparing our approach with the standard one, we remind the reader the idea of the first bottom-up holographic superconductor [6] in Sect. 2. Our SW superconductor is introduced in Sect. 3. Section 4 contains discussions and we conclude in Sect. 5. All plots are presented in Appendix.

2 The simplest standard model of a holographic superconductor

In this Section, we recall the main basic ideas of the first holographic model for the high-T_c superconductivity. This model was constructed as a 3+1 dimensional Einstein gravitational theory with a negative cosmological constant. By assumption, it is dual to a 2+1 dimensional superconductor. The dimensionality was dictated by the experimental fact that the high-T_c cuprates and other high-T_c materials are usually layered and much of the physics is effectively 2+1 dimensional. The model includes a $U(1)$ gauge field interacting (following an analogy with the Landau–Ginzburg theory of superconductivity) with a complex scalar field ψ. The action of the model is [6]

$$S = \int d^4x\sqrt{-g}\left(R + \frac{6}{L^2} - \frac{1}{4}F_{\mu\nu}F^{\mu\nu} - |\nabla\psi - iqA\psi|^2 - m^2\psi^2\right), \tag{1}$$

where R is the scalar curvature, $F_{\mu\nu} = \nabla_\mu A_\nu - \nabla_\nu A_\mu$, L is the AdS radius. The most of the interesting physics appears already in the probe limit: $q \to \infty$ with qA_μ and $q\psi$ fixed. This limit simplifies considerably the model because the backreaction of the fields on the metric is neglected. As a background metric one considers the planar Schwarzschield AdS black hole

$$ds^2 = -f(r)dt^2 + \frac{dr^2}{f(r)} + r^2(dx^2 + dy^2), \tag{2}$$

$$f(r) = \frac{r^2}{L^2}\left(1 - \frac{r_0^3}{r^3}\right). \tag{3}$$

This black hole is invariant under the rescaling

$$r \to \lambda r, \qquad (t, x, y) \to (t, x, y)/\lambda, \qquad r_0 \to \lambda r_0. \tag{4}$$

The Schwarzschield radius r_0 yields the Hawking temperature,

$$T = \frac{3r_0}{4\pi L^2}. \tag{5}$$

The black hole in this model is unstable and forms "scalar hair". To see this one looks for static translationally invariant solutions: $A_r = A_x = A_y = 0$, $A_t = \phi(r)$, $\psi = \psi(r)$. The equations of motion for ϕ and ψ with certain boundary conditions give the relevant solutions. In Ref. [6], the case $m^2 = -2/L^2$ was considered (we will set $L = 1$ in what follows). In this case, the solutions regular at the horizon have the following asymptotics at infinity,

$$\psi = \frac{\psi^{(1)}}{r} + \frac{\psi^{(2)}}{r^2} + \ldots, \qquad \phi = \mu - \frac{\rho}{r} + \ldots, \tag{6}$$

where μ and ρ are interpreted as the chemical potential and charge density of the dual field theory. If we set $\psi^{(1)} = 0$, the behavior of the condensate $\langle O_2\rangle = \psi^{(2)}$ as a function of temperature is depicted in Fig. 1 (see "Appendix"). As $T \to T_c$, the behavior is $\langle O_2\rangle \sim (1 - T/T_c)^{1/2}$ as in the Ginzburg–Landau theory [6].

The plot in Fig. 1 is obtained in the following way. By symmetry, $\psi^{(2)}$ is a function of $r_0/\sqrt{\rho}$. One solves numerically the system of equations of motion at fixed ρ and, using (5), the critical temperature T_c is defined as $\psi^{(2)}(T_c/\sqrt{\rho}) = 0$. Thus, $T_c \sim \sqrt{\rho}$ and one can draw the plot in Fig. 1 in units of T_c.

An important measurable quantity in superconductors is the optical conductivity (the conductivity as a function of frequency). By symmetry, it is enough to analyze the conductivity in the x direction. Consider the perturbations of the vector field in the form

$$A_\mu = A_x(r)e^{i\omega t}. \tag{7}$$

The linearized equation of motion reads

$$A_x'' + \frac{f'}{f}A_x' + \left(\frac{\omega^2}{f^2} - \frac{2\psi^2}{f}\right)A_x = 0. \tag{8}$$

The causal behavior is provided by the ingoing wave boundary condition at the horizon [6],

$$A_x \sim f^{-i\omega/3r_0}. \tag{9}$$

The asymptotic behavior at infinity is

$$A_x = A_x^{(0)} + \frac{A_x^{(1)}}{r} + \dots. \tag{10}$$

Since the behavior (10) holds near the AdS boundary the gauge/gravity correspondence [1,2] tells us that $A_x^{(0)}$ must be identified with the source and $A_x^{(1)}$ is dual to the induced current J_x. Then the definition of the conductivity and the ansatz (7) result in

$$\sigma(\omega) = \frac{J_x}{E_x} = \frac{J_x}{-\dot{A}_x^{(0)}} = \frac{-iA_x^{(1)}}{\omega A_x^{(0)}}. \tag{11}$$

The typical behavior of real and imaginary parts of $\sigma(\omega)$ at $m^2 = -2$ is shown in Figs. 2 and 3. The optical conductivity is constant above T_c, below T_c it develops a gap at some frequency ω_g which can be identified with the minimum of $\mathrm{Im}[\sigma(\omega)]$ [11]. The gap is the most pronounced in the limit $T \to 0$. In this limit $\sqrt{\langle O_2\rangle}/T_c \simeq 7$ (see Fig. 1). In the same limit one can calculate $\omega_g/\sqrt{\langle O_2\rangle} \simeq 1.2$. Both relations turn out to be weakly dependent on the choice of parameters. Excluding $\sqrt{\langle O_2\rangle}$, one arrives at an approximately (within 10 %) universal relation

$$\frac{\omega_g}{T_c} \simeq 8.4. \tag{12}$$

The obtained ration (12) is quite remarkable. First, it is close to that in the high-T_c superconductors [12]. Second, the comparison with the BCS value $\omega_g \simeq 3.5T_c$ shows that the holographic model under consideration seems to describe a system at strong coupling.

Our aim is to construct holographic superconductors without condensates. Such models should respect the scaling symmetry (4) and reproduce a typical behavior of conductivities in the superconducting phase. Below we build some examples for such models.

3 Soft wall holographic superconductor

There exist common features in constructing the bottom-up holographic models for superconductivity and for hadron physics. The solution of equations of motion should yield the optical conductivity in the former case and the correlation functions (with ensuing hadron spectrum) in the latter one. The first bottom-up model for hadrons was proposed in Refs. [13,14]. The action of this model looks like a five-dimensional extension of (1). The condensation of the scalar field ψ described the spontaneous chiral symmetry breaking in QCD. An axial-vector field was also introduced in order to get the chiral dynamics and the mass splitting between the vector and axial mesons. Thus one deals with very similar equations but imposes completely different requirements on the solutions. The important differences in the bottom-up description of hadrons in Refs. [13,14] are as follows: (a) In the probe limit, the background metric is pure AdS (unless one is interesting in some finite-temperature effects); (b) The infrared cutoff r_{IR} is introduced by hands to provide the mass scale (for this reason the model of Refs. [13,14] is referred to as the "hard wall" model); (c) The scalar field ψ condenses first, i.e. the vector fields do not enter the equation of motion for ψ.

The hard wall model describes well the chiral dynamics but gives very rough predictions for the hadron spectrum. In order to improve the second aspect the so-called "soft wall" holographic model was introduced in Ref. [10]. The action of the simplest SW model describing the vector spectrum is

$$S_{\mathrm{SW}} = \int d^5x\sqrt{|g|}\, e^{-2\varphi(ar)}\left(-\frac{1}{4}F_{MN}F^{MN}\right). \tag{13}$$

Now there is no infrared cutoff and the mass scale is provided by the parameter a. The experimental (or theoretically expected) spectrum can be fine-tuned by a choice of the dilaton background φ. Simultaneously, one may reproduce much better the structure of the Operator Product Expansion of the QCD correlation functions. In principle, the dilaton background may be formally (i.e. neglecting a surface term) eliminated by the substitution $A_M \to e^{\varphi}\tilde{A}_M$. The price to pay is the appearance of r-dependent mass term for $\tilde{A}_M$. However, the model can be reformulated in a gauge-invariant way if we assume that this term emerges from condensation of some scalar field ψ [15]. In particular, the standard choice $\varphi \sim r^{-2}$ [10] leads to the (five-dimensional extension of) field part of action (1) with $m^2 = -4$ [15]. In such a "no-wall" model it is assumed that the field ψ condenses first and only after that one analyses the ensuing phenomenology.

We are going to exploit this analogy from the hadron physics as the starting point for construction of a SW holographic superconductor. Discussions of a justification and possible origin of our approach are postponed to Sect. 4.

Consider the gauge-invariant action

$$S = \int d^4x\sqrt{-g}\, e^{-2h\left(\frac{r}{r_0}\right)}\left(-\frac{1}{4}F_{\mu\nu}F^{\mu\nu}\right). \tag{14}$$

The background metric is the black hole one (2). By assumption, the dilaton profile $-2h\left(\frac{r}{r_0}\right)$ emerges due to condensation of some scalar field and satisfies the scaling invari-

ance (4). Making use of the ansatz (7) in the equation of motion, we arrive at the equation

$$A_x'' + \left(\frac{f'}{f} - 2h'\right) A_x' + \frac{\omega^2}{f^2} A_x = 0. \tag{15}$$

As in the "no-wall" model for hadrons, one can eliminate the dilaton background in (14) by the substitution $A_x \to e^h A_x$ and come to the action

$$S = \int d^4x\sqrt{-g}\left\{-\frac{1}{4}F_{\mu\nu}F^{\mu\nu} + \frac{f}{2} \times \left[h'' - (h')^2 + h'\frac{f'}{f}\delta_{ki} + \frac{2h'}{r}\delta_{0i}\right] A_i A^i\right\}, \tag{16}$$

(here $i = 0, 1, 2$; $k = 1, 2$) which is not gauge-invariant in new variable but equivalent to (14). More accurately, the theories (14) and (16) are completely equivalent if the following surface terms are absent,

$$\int d^3x\ \sqrt{-g}\, h' A_0^2\Big|_{r=r_0}^{r=\infty} = 0, \tag{17}$$

$$\int d^3x\ h' f A_k^2\Big|_{r=r_0}^{r=\infty} = 0. \tag{18}$$

Now we can rewrite (16) in the form of (1) with some potential $V(\psi)$ instead of the mass term $m^2\psi^2$. The solution of equation of motion for ψ in the absence of A_μ must reproduce the second term in (16), this dictates the form of the potential $V(\psi)$.

The action (16) leads to the equation of motion

$$A_x'' + \frac{f'}{f}A_x' + \left[\frac{\omega^2}{f^2} + h'' - (h')^2 + h'\frac{f'}{f}\right] A_x = 0. \tag{19}$$

It is easy to check that the substitution $A_x \to e^h A_x$ converts Eqs. (15) to (19). The latter has the form of Eq. (8). The term containing ψ in Eq. (8), which was a numerical solution of coupled system of equations in Ref. [6], is replaced in Eq. (19) by a term completely dictated by the function h. We are free to choose this function phenomenologically.

Consider the possibilities $h = r_0/r$ and $h = (r_0/r)^2$, where the scaling (4) is taken into account. They correspond to solutions with condensates $\langle O_1\rangle$ and $\langle O_2\rangle$ in (6). The resulting behavior of optical conductivities $\sigma(\omega)$ is displayed in Figs. 4 and 5, respectively. The obtained shapes recover (at least qualitatively) the results of Ref. [6]. These two differing shapes are expected for superconductors having the so-called type II and type I coherence factors.

The considered possibilities can be generalized to the ansatz

$$h = \alpha\left(\frac{r_0}{r}\right)^\beta. \tag{20}$$

We may vary the parameter α at fixed β and vice versa and look at the behavior of optical conductivity. A couple of corresponding examples are demonstrated in Figs. 6, 7 and 8, 9, respectively. A non-polynomial ansatz for h can be chosen. An example is presented in Figs. 10 and 11.

The plots of $\mathrm{Re}[\sigma(\omega)]$ in Fig. 6 show a formation of gap with changing α. This suggests that in reality α should be a decreasing function of T, say a positive power of $(1 - T/T_c)$. The parameter β may also include a temperature dependence with some critical value, moreover, it might be responsible for the coherence factor type.

The main lesson of the exercises above is that given a concrete superconducting material, in principle, one is able to find phenomenologically the form of the dilaton background h that interpolates the observable superconducting properties of this material. Then one can use the obtained h to interpolate the properties of other known high-T_c superconductors and reveal the required change of input parameters. This would help to ascribe a physical meaning to the model parameters. Next step would be a derivation of a phenomenologically reasonable form(s) of h from a consistent gauge/gravity theory. As usual, this step is the most difficult.

In the probe limit, the form of the dilaton profile $-2h\left(\frac{r}{r_0}\right)$ should follow from an action

$$S_\varphi = \int d^4x\sqrt{-g}\left(-\frac{1}{2}\partial_\mu\varphi\partial^\mu\varphi - V(\varphi)\right), \tag{21}$$

with the black hole metric (2). A solution of equation of motion should yield $\langle\varphi\rangle \equiv h$. The potential $V(\varphi)$ can be restored from the form of $h\left(\frac{r}{r_0}\right)$. For instance, if we choose $2h = \left(\frac{r}{r_0}\right)^\beta$ then

$$V = \beta\left[\frac{1}{2}(\beta+3)\varphi^2 - \frac{\beta^2 r_0^3}{2-3/\beta}\varphi^{2-3/\beta}\right]. \tag{22}$$

Imposing the Breitenlohner–Freedman boundary for the scalar mass in the AdS_{d+1} space-time [16], $m^2 \geq -\frac{d^2}{4L^2}$, we have $\beta(\beta+3) \geq -9/4$ that leads to $(\beta - 3/2)^2 \geq 0$, i.e. any value of β is allowed, with the value $\beta = -3/2$ providing the minimal mass. The second term in (22) looks unnatural since it emerges due to the horizon and contains a non-integer power of interaction except some special cases. This situation is quite general. If we take the point of view that in the holographic approach, which is inherently large-N one, only quadratic in fields part is relevant, then we should either assume $r_0 = 0$ in (22), i.e. somehow motivate pure AdS metric in (21), or exclude the interaction term. In the latter case, the equation of motion for $\varphi = \varphi(r)$,

$$-\left(r(r^3 - r_0^3)\varphi'\right)' + r^2\beta(\beta+3)\varphi = 0, \tag{23}$$

has solutions in terms of the Legendre functions of the first (P) and second (Q) kind,

$$\varphi^{(1)} = P_{\beta/3}\left(1-\frac{2r^3}{r_0^3}\right), \qquad \varphi^{(2)} = Q_{\beta/3}\left(1-\frac{2r^3}{r_0^3}\right). \tag{24}$$

The energy functional of the action (21) is minimal at $\beta = -3/2$. Accepting this value we observe that the solution $\varphi^{(1)}$ is irregular at the horizon while choosing $h = Q_{-1/2}(1-2(r/r_0)^3)$ in (14) we obtain a realistic prediction for the optical conductivity which is depicted as one of plots in Figs. 12 and 13.

For comparison, we reproduce in Fig. 14 a certain experimental plot for $\mathrm{Re}[\sigma(\omega)]$ demonstrating the difference of the shape below and above the critical temperature T_c. It is seen that in reality the parameter β in (22) should depend on T achieving a critical value between $\beta/3 = -0.7$ and $\beta/3 = -0.75$ where the local minimum in $\mathrm{Re}[\sigma]$ disappears. In contrast to the Ginzburg–Landau theory, the quadratic part of the potential (22) does not vanish at the critical point. This feature could have a natural interpretation – the high-T_c superconductors represent doped materials and their T_c depends crucially on the density of doped holes x that lies in a finite interval $a < x < b$ [7]. The maximal T_c roughly corresponds to $x = (a+b)/2$ (the optimal doping). Thus the parameter β in (22) might encode a dependence on the doping x.

4 Discussions

The presented approach to building a bottom-up holographic superconductor is more phenomenological than the original one [6]. As in Ref. [6], our original action (14) is gauge-invariant, however, it can be useful to rewrite (14) in a gauge-noninvariant form (16) via a change of variables. By assumption, our model is formulated for the superconducting phase and does not describe a transition to this phase. A question appears whether the model describes a high-T_c superconductor rather than merely more generic features of $2+1$ dimensional strongly coupled materials? For instance, the optical conductivity measured in graphene behaves very similar to Figs. 2 and 3 [3]. It is not excluded that the answer to this question is positive. In this regard it is interesting to mention that the phase transition in graphene is of topological nature, i.e. it is related with a change of topology of Fermi surface and has nothing to do with some spontaneous symmetry breaking and an order parameter. As we discussed in Introduction, the mechanism of phase transition in high-T_c materials seems to be quite complicated and it hardly can be described by any simple model. But if we consider a more modest problem – the behavior of a system after the phase transition (as we did) – this behavior may indeed reveal some universal features for very different systems.

A holographic description of a genuine superconductor should include a gauge symmetry on the boundary, i.e. dynamical photons. Otherwise the models like in Ref. [6] describe a charged superfluid rather than a superconductor. In our case, one should add an external electromagnetic field with a coupling to dilaton. Following Ref. [9], after integrating out all other degrees of freedom one can find the effective photon mass and determine the type of superconductor. This analysis is left for future.

It would be interesting to clarify a possible origin of our approach. The SW holographic model in hadron physics cannot help because its relation to any fundamental string theory is unknown. The full action for the considered holographic superconductor is

$$S = \kappa_1 S_{\mathrm{grav}} + \kappa_2 S_\varphi + \kappa_3 S_{\varphi,A}. \tag{25}$$

Our approach is justified if

$$\kappa_1 \gg \kappa_2 \gg \kappa_3. \tag{26}$$

By assumption, the part $\kappa_1 S_{\mathrm{grav}}$ gives the black hole metric (2) and the backreaction to the metric from $\kappa_2 S_\varphi$ and $\kappa_3 S_{\varphi,A}$ can be neglected due to (26). After that we find $\langle\varphi\rangle$ from minimum of S_φ and then extract the phenomenology from $S_{\varphi,A}$. In principle, the condition $\kappa_2 \gg \kappa_3$ is not necessary but it guarantees the absence of solutions where both φ and A are equally small and that such solutions do not give an absolute minimum to the energy.

Following the analogy with the SW model in hadron physics [10], we have chosen the interaction of the scalar field φ with the gauge field A in the form $e^{\varphi}F_{\mu\nu}^2$. In principle, such coupling is provided by some known dilatonic black holes unstable to forming the scalar hair [4]. However, this possibility has not been exploited in holographic superconductors because $F_{\mu\nu}^2$ acts as a source for φ, so $\langle\varphi\rangle \neq 0$ for any charged black hole [4]. In our case, the given argument does not apply since, first, φ in the exponent represents a fixed background, second, we are free to choose a different coupling, say, $e^{\varphi^2}F_{\mu\nu}^2$.

How the action (25) with the sequence of scales (26) may follow from a string theory is an open problem. In the case of holographic dual for a conformal $SU(N)$ gauge theory, one has $\kappa_1 = \mathcal{O}(N^2)$. We may implement (26) assuming the scaling

$$\kappa_1 = \mathcal{O}(N^2), \qquad \kappa_2 = \mathcal{O}(N), \qquad \kappa_3 = \mathcal{O}(1), \tag{27}$$

at large N. This scaling entails the question about the physical meaning of N in the holographic superconductors. The

given question is tightly related with a long standing problem concerning the analog of large-N limit in condensed matter systems [4].

Perhaps the answer lies in the structure of high-T_c superconductors. They represent small pieces of layered materials [12]. Imagine that N is the number of layers. Imagine further that each layer interacts with all (or a substantial part of) other layers. Then we have $\mathcal{O}(N^2)$ interactions and the corresponding background medium is described in the action (25) by the part $\kappa_1 S_{\rm grav}$ with $\kappa_1 = \mathcal{O}(N^2)$. Since in the experimental patterns the layers are weakly coupled [4], we should have a weakly coupled gravitational theory as it is required by the AdS/CFT correspondence. Assume that the medium inside each layer can be modelled by a relativistic theory of the scalar field φ. Since we have N layers, in (25) the contribution S_φ emerges with $\kappa_2 = \mathcal{O}(N)$. The real high-$T_c$ materials can have several sorts of layers composed of different atoms. So, strictly speaking, we should consider several fields φ_i. But we simplify the situation. The part $\kappa_3 S_{\varphi,A}$ describes a response of the system to the electromagnetic field. This response is unrelated to the number of layers, thus $\kappa_3 = \mathcal{O}(1)$.

The outlined physical picture could justify the choice of the action (25) with the behavior of constants (27) at large N. In some sense, within this interpretation a layered material resembles the stack of N branes in the AdS/CFT correspondence [17]. Such a resemblance might be among reasons why the gauge/string duality can be successfully applied to the high-T_c superconductors.

In our approach, the dilaton profile comes from condensation of a scalar field. This description should be dual to a theory of S-wave superconductors. Many real high-T_c superconductors are known to have the D-wave (the cuprates) or sometimes P-wave superconductivity [12]. The construction of the corresponding extensions is straightforward – one should replace the contribution S_φ in (25) by an action for the vector or tensor field that condenses and forms the dilaton profile in $S_{\varphi,A}$. In principle, the vector or tensor condensate can be made anisotropic and, hence, describe the anisotropic (striped) superconductivity.

5 Conclusions

In the present work, we have made an attempt to advance in the quantitative holographic description of the high-T_c superconductors. For this purpose we applied the idea of the soft wall holographic model from hadron physics [10]. The phenomenological description of the form of the optical conductivity in our approach is in one-to-one correspondence with the phenomenological description of the form of the hadron spectrum in the standard SW model [10]. The simplest model of holographic superconductor is believed to be the one proposed in the original paper [6]. We have shown that for this purpose it is possible to construct models which are technically simpler. In our approach, the conductivity follows from a solution of one differential equation instead of system of two coupled differential equations in Ref. [6]. This technical simplicity is likely the main advantage of the proposed SW holographic superconductors. As to conceptual points – understanding the origin of our model and its possible derivation from some string theory – our approach is of course not simpler.

In hadron physics, the SW model does not describe (without significant complications) the dynamics of the chiral symmetry breaking but in description of the observable spectrum it seems to be the most successful bottom-up holographic approach. In the holographic superconductors, we have a similar situation: The considered SW model (in its current form) does not describe the phase transition to superconductivity, but if we are interested in the experimentally measurable quantities like optical conductivity, the SW superconductors are able to describe the emerging phenomenology more realistically than many other holographic superconductors.

There are various directions for extensions and applications of the proposed approach. We mention some of them. (i) It would be interesting to identify the most reasonable dilaton profiles from the best fit to the experimental data on the optical conductivities. (ii) One can calculate other transport properties and study the response to the non-zero chemical potential and (electro)magnetic field. (iii) At some choices of the dilaton profile the SW model seems to describe a superinsulator and this could be interesting. (iv) Perhaps the phase transition to superconductivity can be modelled as the Hawking-Page phase transition in the gravitational part of (25) from the thermal AdS space to AdS with black hole [18]. The transition point could relate the critical temperature to some dimensional model parameter (as in Ref. [19] for the deconfinement temperature). (v) Among theoretical challenges for the holographic superconductors one can mention the problem of a dual gravitational interpretation for the empirical Homes' scaling law in the high-T_c superconductors [20] (see [21,22] for a discussion from the holographic perspective). Our preliminary analysis showed that this law imposes rather strong constraint on the mutual dependence of the model parameters and seems to prescribe for them a certain temperature dependence. We hope to address at least some of the issues above in the future work.

Acknowledgments The authors acknowledge Saint Petersburg State University for research Grant 11.38.189.2014. The work was also partially supported by the RFBR Grant 16-02-00348-a.

Funded by SCOAP[3].

Appendix: Plots

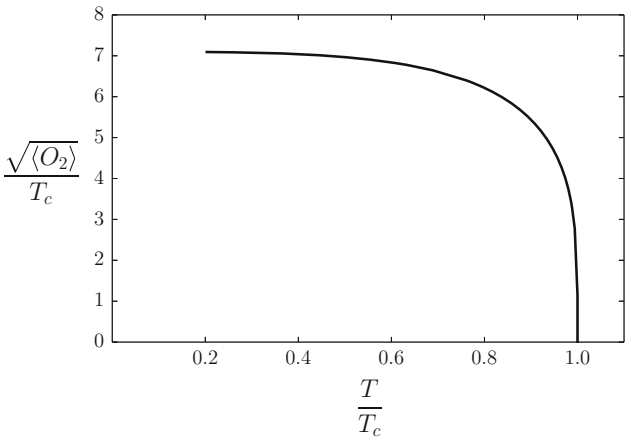

Fig. 1 The condensate $\langle O_2\rangle$ as a function of temperature for $m^2 = -2$ [5]

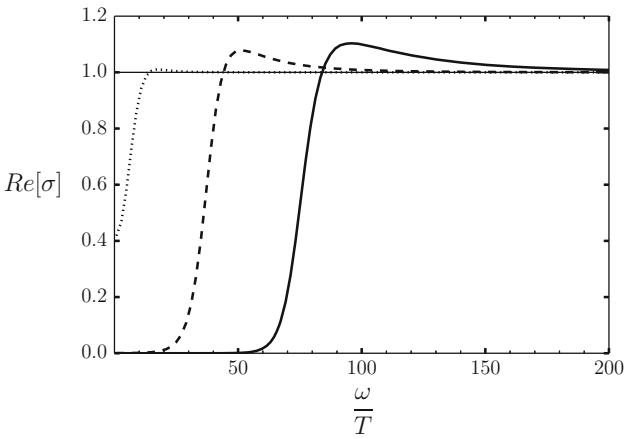

Fig. 2 The real part of the optical conductivity as a function of frequency normalized by temperature for $m^2 = -2$. Curves from *left* to *right* correspond to $\frac{T}{T_c} = \lambda \approx 0.888$ (*dotted*), $\lambda \approx 0.222$ (*dashed*) and $\lambda \approx 0.105$ (*solid*) [5]

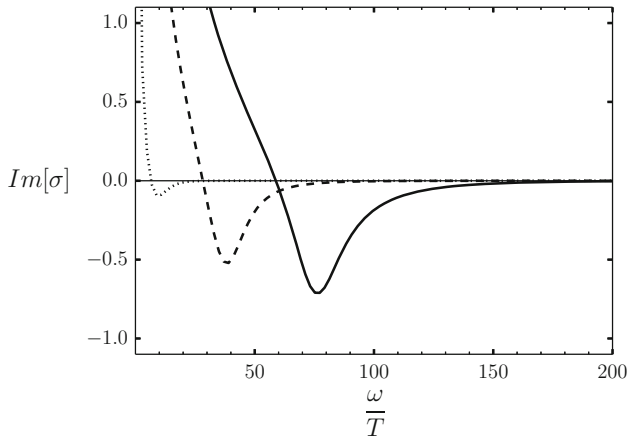

Fig. 3 The imaginary part of the optical conductivity from Fig. 2 [5]

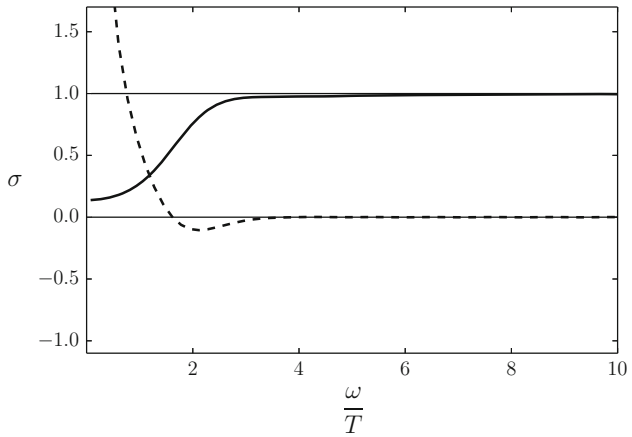

Fig. 4 The optical conductivity at $h = r_0/r$. The *solid line* corresponds to Re[σ] and the *dashed one* to Im[σ]

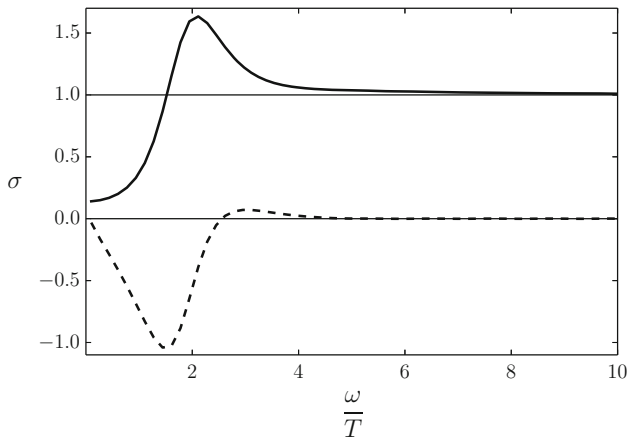

Fig. 5 The optical conductivity at $h = (r_0/r)^2$. The notations are as in Fig. 4

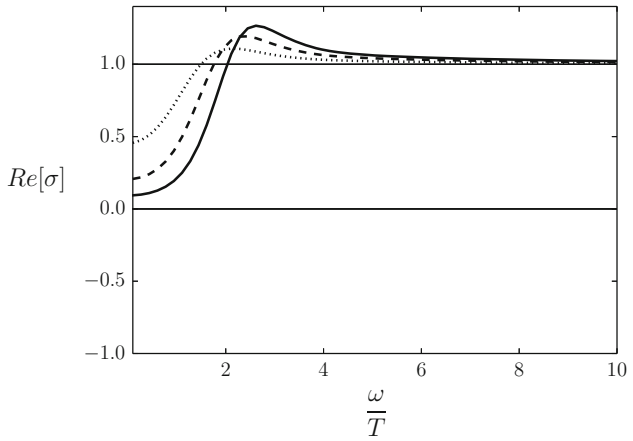

Fig. 6 Re[σ] at $h = \alpha \left(\frac{r_0}{r}\right)^{1.4}$. From left to right $\alpha = 0.4$ (*dotted*), $\alpha = 0.8$ (*dashed*) and $\alpha = 1.2$ (*solid*)

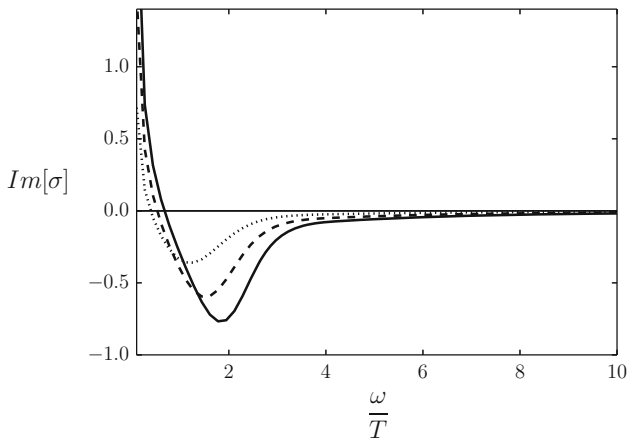

Fig. 7 Im[σ] corresponding to the plots in Fig. 6

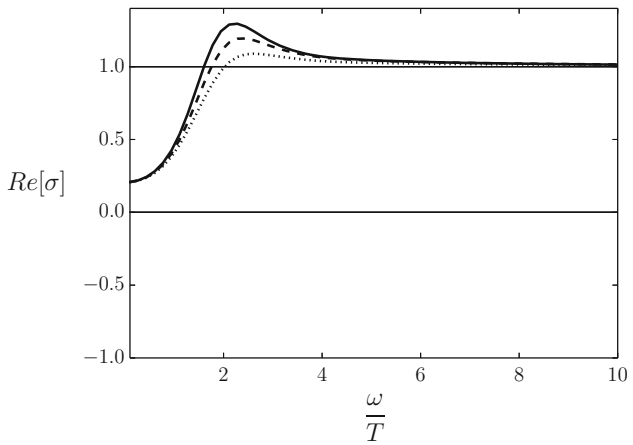

Fig. 8 Re[σ] at $h = 0.8 \left(\frac{r_0}{r}\right)^{\beta}$. From *right* to *left* $\beta = 1.2$ (*dotted*), $\beta = 1.4$ (*dashed*) and $\beta = 1.6$ (*solid*)

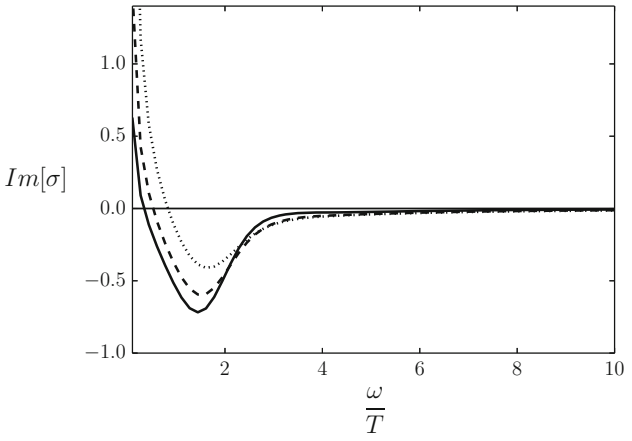

Fig. 9 Im[σ] corresponding to the plots in Fig. 8

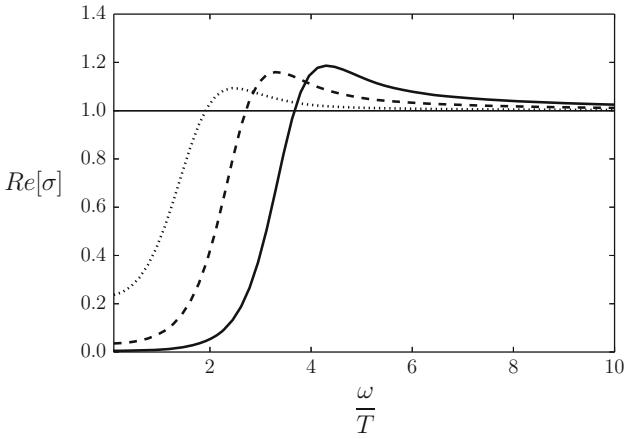

Fig. 10 Re[σ] at $h = \log\left(\cosh\left(\frac{1}{2} + \alpha \frac{r_0}{r}\right)\right)$. From *left* to *right* we take $\alpha = 1$ (*dotted*), $\alpha = 2$ (*dashed*) and $\alpha = 3$ (*solid*)

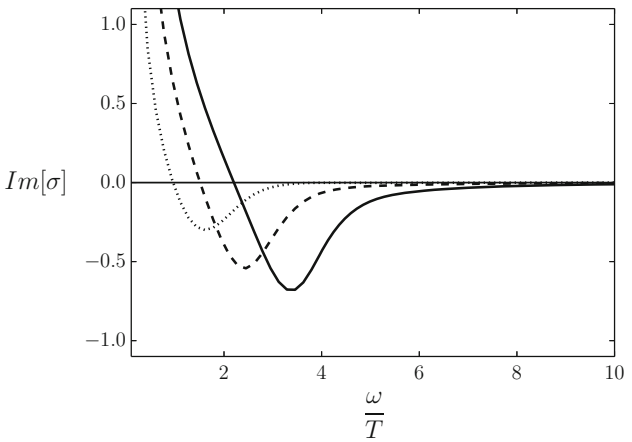

Fig. 11 Im[σ] corresponding to the plots in Fig. 10

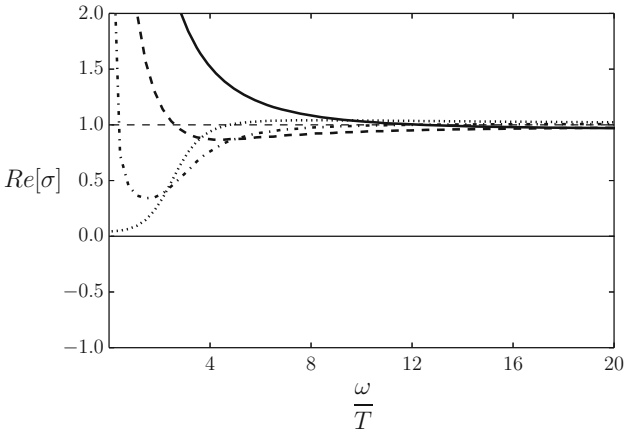

Fig. 12 Re[σ] at $h = Q_v(1-2(r/r_0)^3)$. From *left* to *right* $\nu = -0.5$ (with an approximate δ-function at $\frac{\omega}{T} = 0$), $\nu = -0.6$, $\nu = -0.7$, $\nu = -0.75$

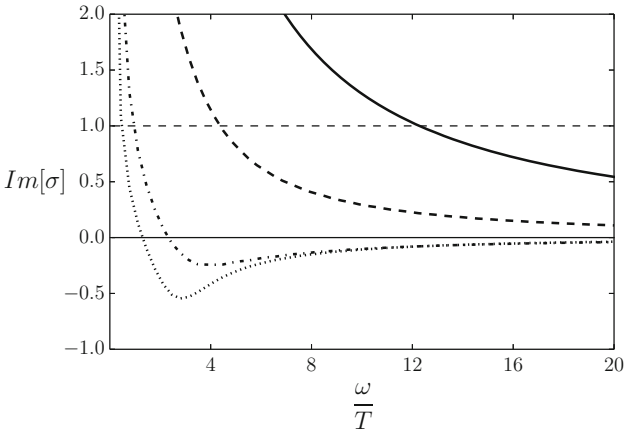

Fig. 13 Im[σ] corresponding to the plots in Fig. 12

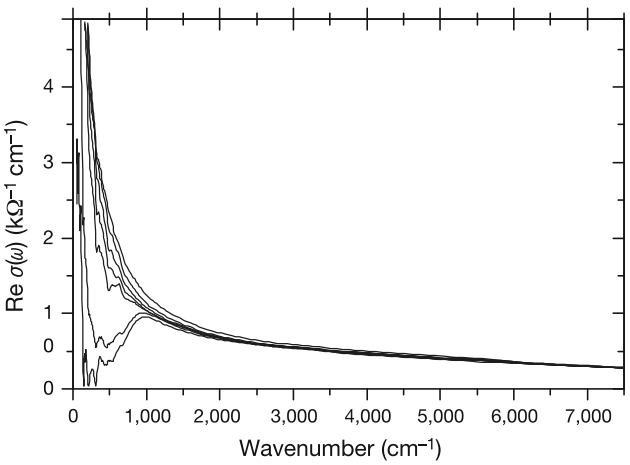

Fig. 14 The real part of the optical conductivity along the copper–oxygen planes of $Bi_2Sr_2Ca_{0.92}Y_{0.08}Cu_2O_{8+\delta}$ for a selected number of temperatures. Temperatures from *left* to *right* are 7, 50, 95, 130, 160, 200, 260 K. The critical temperature is 96 K. Experimental plot from Ref. [23]

References

1. E. Witten, Adv. Theor. Math. Phys. **2**, 253 (1998)
2. S.S. Gubser, I.R. Klebanov, A.M. Polyakov, Phys. Lett. B **428**, 105 (1998)
3. S.A. Hartnoll, Class. Quantum Gravity **26**, 224002 (2009)
4. G.T. Horowitz, Lect. Notes Phys. **828**, 313 (2011)
5. R.G. Cai, L. Li, L.F. Li, R.Q. Yang, Sci. China Phys. Mech. Astron. **58**, 060401 (2015)
6. S.A. Hartnoll, C.P. Herzog, G.T. Horowitz, Phys. Rev. Lett. **101**, 031601 (2008)
7. E.W. Carlson, V.J. Emery, S.A. Kivelson and D. Orgad arXiv:cond-mat/0206217
8. A.J. Leggett, Nature Phys. **2**, 134 (2006)
9. S.A. Hartnoll, C.P. Herzog, G.T. Horowitz, JHEP **0812**, 015 (2008)
10. A. Karch, E. Katz, D.T. Son, M.A. Stephanov, Phys. Rev. D **74**, 015005 (2006)
11. G.T. Horowitz, M.M. Roberts, Phys. Rev. D **78**, 126008 (2008)
12. K.K. Gomes et al., Nature **447**, 569 (2007)
13. J. Erlich, E. Katz, D.T. Son, M.A. Stephanov, Phys. Rev. Lett. **95**, 261602 (2005)
14. L. Da Rold, A. Pomarol, Nucl. Phys. B **721**, 79 (2005)
15. S.S. Afonin, Int. J. Mod. Phys. A **26**, 3615 (2011)
16. P. Breitenlohner, D.Z. Freedman, Ann. Phys. **144**, 249 (1982)
17. O. Aharony et al., Phys. Rep. **323**, 183 (2000)
18. S.W. Hawking, D.N. Page, Commun. Math. Phys. **87**, 577 (1983)
19. C.P. Herzog, Phys. Rev. Lett. **98**, 091601 (2007)
20. C.C. Homes et al., Nature **430**, 539 (2004)
21. J. Erdmenger, P. Kerner, S. Muller, JHEP **1210**, 021 (2012)
22. J. Erdmenger, B. Herwerth, S. Klug, R. Meyer, K. Schalm, JHEP **1505**, 094 (2015)
23. D. van der Marel et al., Nature **425**, 271 (2003)